Available online at www.sciencedirect.com

ScienceDirect

Ceramics International 41 (2015) 10051–10056

CERAMICS INTERNATIONAL

www.elsevier.com/locate/ceramint

Synthesis and characterization of potassium hexatitanate using boric acid as the flux

P. Ponce-Peña[a], M.A. González-Lozano[a,*], M.A. Escobedo-Bretado[a], P. de Lira-Gómez[b], E. García-Sánchez[b], E. Rivera[c], L. Alexandrova[c]

[a]*Facultad de Ciencias Químicas de la Universidad Juárez del Estado de Durango, Av. Veterinaria S/N, Circuito Universitario, C.P. 34120 Durango, Dgo., Mexico*
[b]*Universidad Autónoma de Zacatecas, Jardín Juárez 147, Centro Histórico, C.P. 98000 Zacatecas, Zacatecas, Mexico*
[c]*Instituto de Investigación en Materiales de la UNAM, Circuito Exterior, Ciudad Universitaria, Coyoacán, 04510 México D. F., Mexico*

Received 22 January 2015; received in revised form 15 April 2015; accepted 17 April 2015
Available online 25 April 2015

Abstract

In this study, the viability of obtaining potassium hexatitanate fibers ($K_2Ti_6O_{13}$) via the flux method using boric acid subjected to different melting temperatures and cooling media (air or water) was investigated. According to the results, the amount of used flux enabled the production of a liquid phase in which the TiO_2 and K_2O reacted to form $K_2Ti_6O_{13}$ with various morphologies. The melting temperature did not significantly influence the microstructure presented by the materials; however, an amorphous phase with small crystals was obtained when molten mixtures were poured into water in comparison with the samples cooled with air. With the goal of obtaining homogeneous fibers, the samples with lower crystallinity (poured into water) were heated at 900, 950 and 1000 °C. Fibers were produced with sizes varying from 12 to 35 μm in length and 0.51–0.90 μm in diameter as well as with a large specific surface area and a band gap value of 3.3 eV; these characteristics make these fibers promising for use as photocatalysts.

Keywords: Potassium hexatitanate; Flux method; Photocatalyst

1. Introduction

Potassium titanates with the chemical formula of $K_2O \cdot nTiO_2$, with $n=2$, 4, 6, 8 are important functional materials that exhibit unique crystalline structures and a wide variety of industrial applications, such as ionic exchangers filters, electric insulators, photocatalysts and reinforcing agents in polymers, metals and ceramics [1–3]. In particular, potassium hexatitanate ($K_2Ti_6O_{13}$) has the following characteristics: an acicular morphology, a high melting point (1370 °C), a tunnel-like structure that confers it good properties as a thermal insulator, and a high chemical stability. Recently, a good photocatalytic activity in the split water reaction [4,5] has been demonstrated using this material.

The most common methods for $K_2Ti_6O_{13}$ production are calcination (and calcination with slow cooling), hydrothermal reactions, flux evaporation, flux growth, ionic exchange and molten salts. Usually, potassium carbonate (K_2CO_3) and titanium dioxide (TiO_2) are starting materials that react at high temperatures [1,2,6–8]. The flux growth method has been extensively investigated and has been shown to provide fine single crystals of small size, depending on the synthesis conditions. In recent years, this method has been applied for the preparation of inorganic crystals as photocatalysts, such as TiO_2 [9], $Na_2Ti_6O_{13}$ [10], $K_2Ti_6O_{13}$ [11], and so on. Many fluxes, such as K_2MoO_4, Li_2O-K_2MoO_4, K_2O–MoO_3, K_2O–WO_3, PbO, Bi_2O_3, K_2CO_3–$K_4P_2O_7$, K_2CO_3–V_2O_5, PbO–$K_4P_2O_7$ and KCl–KF have been used. However, a disadvantage of these materials is that they are expensive and/or corrode the container in which they are molten [8,12,13]. In this sense, the use of B_2O_3 as a flux, as a mixture of K_2O–B_2O_3–Na_2O, has been only reported by Kajiwara [13]. For this purpose, the

*Corresponding author. Tel.: +52 618 1301120; fax: +52 618 1301111.
E-mail address: magl62001@yahoo.com.mx (M.A. González-Lozano).

http://dx.doi.org/10.1016/j.ceramint.2015.04.093
0272-8842/

study of cheap alternative fluxes allowing for decreasing costs to obtain $K_2Ti_6O_{13}$ fibers is interesting. This study considers the viability of synthesizing $K_2Ti_6O_{13}$ fibers using boric acid as a flux, varying the melting temperature and the method of cooling (in steel plate or water), and determines if these materials could act as photocatalysts in the UV–vis range.

2. Materials and methods

2.1. Materials

Raw materials (purity > 99%), TiO_2 (Sigma-Aldrich), K_2CO_3 (Fermont) and H_3BO_3 (Fermont) were used as a flux. Two cooling media were used: a steel plate (cooling with air at room temperature) and water at room temperature. In this case, the faster the variation of the cooling conditions, the smaller the size of the obtained crystals.

Table 1
Investigated compositions.

Sample	Composition (% mol)			Melting temperature (°C)	Cooling media	Heat treatment (°C)
	K_2O	TiO_2	B_2O_3			
1VP1250	30	55	15	1250	Air	–
1VA1250				1250	Water	–
1VP1300				1300	Air	–
1VA1300				1300	Water	–
2VP1250	30	60	10	1250	Air	–
2VA1250				1250	Water	900 (M1), 950 (M2), 1000 (M3)
2VP1300				1300	Air	
2VA1300				1300	Water	900 (M4), 950 (M5), 1000 (M6)

2.2. Preparation of $K_2Ti_6O_{13}$

In this work, two compositions reported by González Lozano et al. [14], which produce glass–ceramics with a potassium hexatitanate phase, were used. Table 1 presents the investigated compositions, temperature and cooling conditions used in each composition. Mixtures of raw materials were molten in a platinum crucible in an electrical furnace (Lindberg Blue BF51433). The furnace program included heating up to 400 °C (to decompose boric acid and avoid losses due to volatilization [15]), which was maintained for 1 h, followed by heating up to 1250 or 1300 °C and maintaining the temperature for another hour. Each of the melts were poured onto a steel plate (cooling on air, designed as VP) or into water (designed as VA). After cooling, the samples were powdered into an agate mortar (−80 mesh, 180 μm), and then, the remnant flux was dissolved in hot water (95 °C) using a ratio of powder:water of 1:20 [14] under magnetic stirring at a rate of 150 rpm for two hours. Finally, the solutions were filtered, and then, the powders were dried at 70 °C for two hours.

Likewise, with the goal of preparing homogeneous fibers, powders obtained from compositions 2VA1250 and 2VA1300 (which exhibited poor crystallinity according to the XRD results) were each thermally treated at 900, 950 and 1000 °C for 2 h, using a heating rate of 10 °C/min. The six samples obtained here were named M1–M6 (see Table 1).

2.3. Characterization

The crystalline phases for all of the samples, both before and after dissolution treatment, were analyzed by X-ray diffraction (XRD, Philips X'Pert-MPD) using Cu-Kα radiation, with the peaks identified by means of the ICDD standard database. Likewise, the powdered samples were attached to a metallic cylinder and coated with graphite and then characterized using a scanning electron microscope (SEM, Philips XL30ESEM) equipped with an X-ray

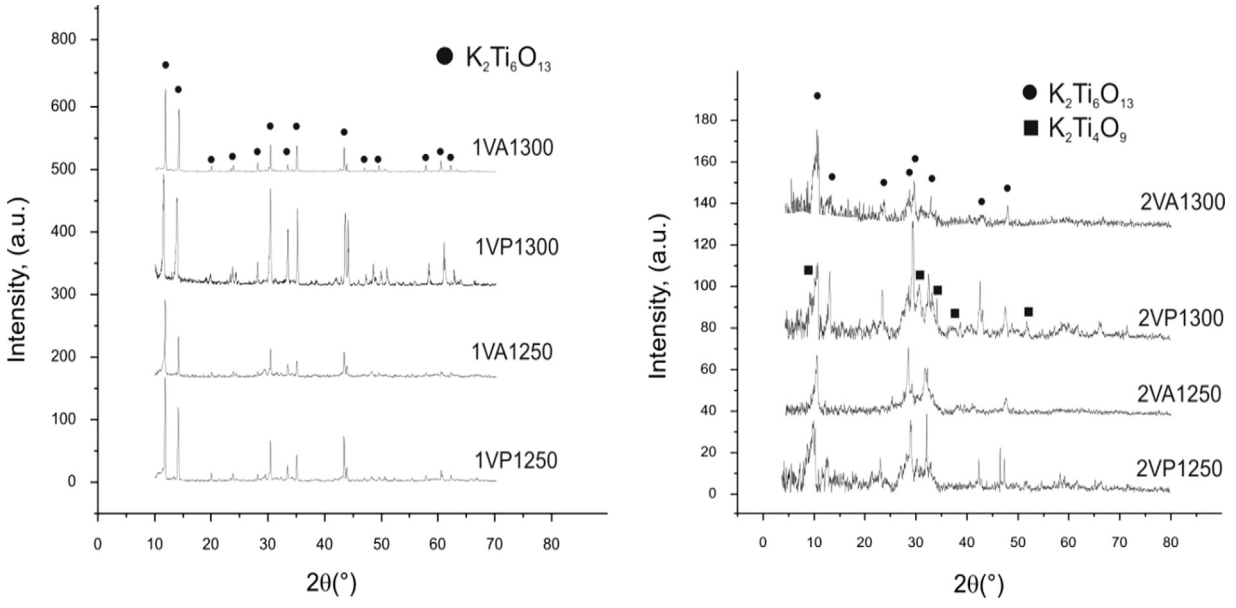

Fig. 1. XRD patterns of all of the investigated compositions.

micro-analyzer for energy dispersive spectroscopy (EDS, EDAX Pegasus).

Samples M1–M6 were characterized using XRD and SEM. Similarly, the Brunauer–Emmett–Teller (BET) specific surface area was calculated from the amount of N_2 adsorption at 77 K, which was measured using a Quantachrome Instrument. Diffuse reflectance DR UV–visible (DR UV–vis) spectra were recorded at room temperature using a JASCO V-570 equipped with an integrating sphere; the Kubelka Munk function was calculated from absorption data from diffuse reflectance, and the band gap values were calculated by extrapolating the linear part of the Kubelka Munk function graphics to the *x*-axis, corresponding to the measured energy in eV (Kubelka Munk vs. Energy) [16]. The Kubelka–Munk function, $F(R)$, is given by the following equation:

$$F(R) = \frac{(1-\mathrm{R})^2}{2\mathrm{R}} \quad (1)$$

where R is the diffused reflectance at a given wavelength.

3. Results and discussion

3.1. Characterization of samples without heat treatment

All of the investigated compositions were found to be fused and could be poured. The XRD patterns of all of the samples are shown in Fig. 1; the peaks were indexed and compared with the ICDD cards. In Composition 1, $K_2Ti_6O_{13}$ (01-074-0275) corresponds to a single phase, whereas Composition 2 corresponds to a mixture of $K_2Ti_6O_{13}$ and $K_2Ti_4O_9$ (00-013-0447). Some materials are well known to be prepared in such a way that they give a mixture of crystalline and amorphous phases; in these cases, the crystallinity is normally specified as a percentage of the total volume of the material that is crystalline. As shown in Fig. 1, the powders of Composition 1 exhibited higher crystallinity (intense diffraction peaks) in comparison with the powders of Composition 2. We suggest that with higher flux amounts (15% of B_2O_3), there is enough molten flux to favor the dissociation of the starting materials at low temperature (lower than melting point of the $K_2Ti_6O_{13}$). The

Table 2
Relative crystallinity of the samples.

Sample	Most intense peak (counts)	Relative crystallinity
1VP1250	173	97.0
1VA1250	120	68.6
1VP1300	175	100
1VA1300	135	79.4
2VP1250	36	20.6
2VA1250	28	16.0
2VP1300	38	21.7
2VA1300	38	21.7

Table 3
EDS microanalysis of the glassy and crystalline phases.

EDS	Atomic (%)			
	O	K	Ti	B
Spectrum 1	58.55	7.65	1.35	32.43
Spectrum 2	69.32	7.73	22.95	0.0
Spectrum 3	61.38	6.66	1.03	30.93
Spectrum 4	64.20	8.50	27.30	0.0
Spectrum 5	62.18	8.34	1.05	28.43
Spectrum 6	63.62	8.78	27.60	0.0
Spectrum 7	60.81	9.03	0.83	29.33
Spectrum 8	65.39	8.81	25.80	0.0

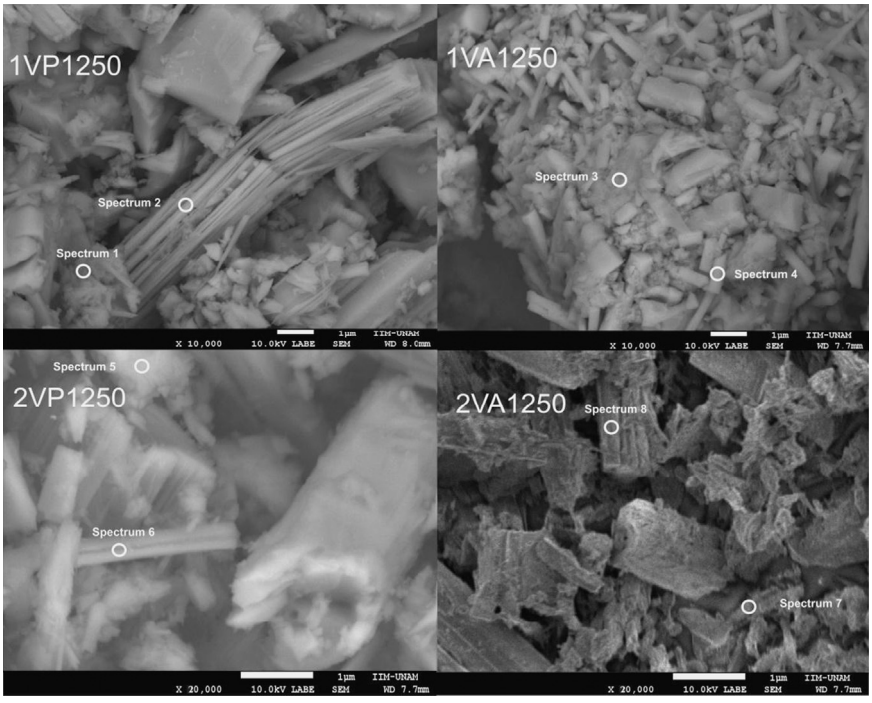

Fig. 2. Microstructure of the 1VP1250, 1VA1250, 2VP1250 and 2VA1250 samples before dissolution treatment.

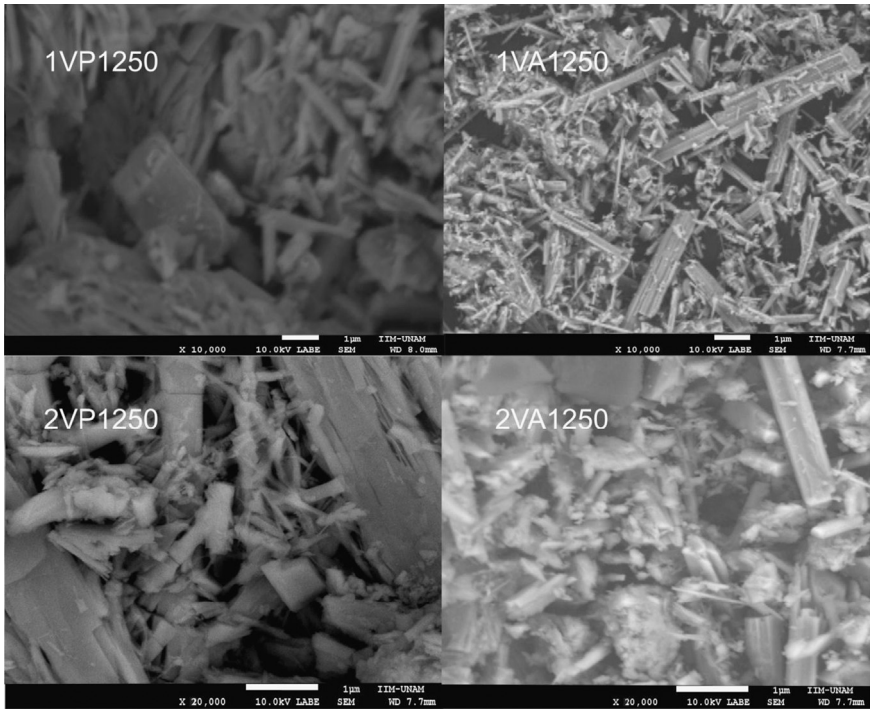

Fig. 3. Microstructure of the 1VP1250, 1VA1250, 2VP1250 and 2VA1250 samples after the dissolution-filtering process.

presence of TiO_2 and K_2O species (which enhance diffusion and mass transport) facilitate the crystallization of $K_2Ti_6O_{13}$ during the cooling stage. In addition, in both compositions, the samples poured in water clearly exhibited lower crystallinity in comparison with the samples cooled with air. This lower crystallinity can be observed as a decrease in the intensity of the peaks present in the diffractograms. Comparison of the crystallinity of the samples was performed by taking the material that presented the most intense peak at ~11.5 ($2\theta(^\circ)$), which was assigned the relative value of 100%, as a reference. Therefore, the composition of 1VP1300 was found to be the most crystalline, whereas the 2VA1250 composition exhibited the lowest crystallinity (Table 2).

Fig. 2 shows the microstructures of the obtained materials after pouring. The melting temperature did not significantly influence the microstructure presented by these materials, and only the melts resulted in more fluid (eye evaluated) when they were cast. However, smaller crystals were obtained when the molten samples were cooled with water, in comparison with the samples cooled with air. This result reflects the higher cooling rate that was enabled by the more rapid heat dissipation that occurred because of the division of the molten mixtures into many parts, which are in contact with water. The faster the variation of the cooling conditions, the smaller the size of the obtained crystals; the material can even present amorphous phases under such conditions. According to Yoshida et al. [5], this process of cooling can promote a number of defects on the surface of the $K_2Ti_6O_{13}$ fibers produced by the flux method. On the contrary, this defect formation does not occur when melts are cooled with air because the obtained crystals present smooth surfaces, such as those observed in the materials prepared in this work.

The obtained materials can be referred to as glass–ceramics because they have one or two crystalline phases (potassium titanates) and a glassy phase in which the crystals are embedded. The glassy phase consists primarily of B_2O_3 and K_2O, with a small amount of TiO_2 (borate glass); this composition was confirmed by EDS semi-quantitative analysis, as shown in Table 3. It is proposed that the glassy phase of Composition 2 (15% B_2O_3) allows the introduction of a higher amount of K_2O in the glass network, leaving fewer spaces available to be combined with the TiO_2 and to crystallize into the $K_2Ti_6O_{13}$ phase (with the higher molar ratio TiO_2:K_2O of 6:1) compared with Composition 2 (10% B_2O_3), which favored the formation of two crystalline phases: $K_2Ti_6O_{13}$ and $K_2Ti_4O_9$ with a lower molar ratio of TiO_2:K_2O of 4:1.

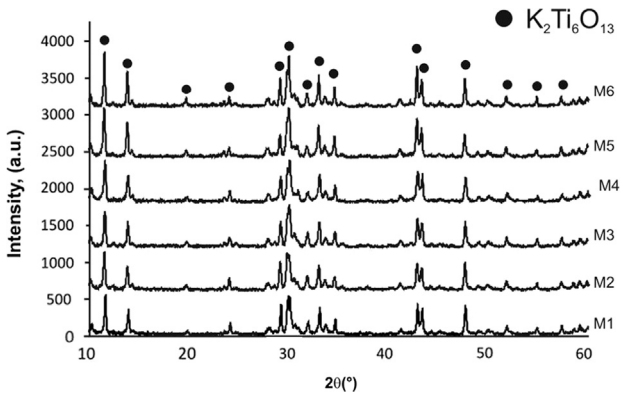

Fig. 4. Difractograms of samples M1–M6.

However, borate glasses are well known to have high water solubility, with the dissolution process being controlled by the hydrolysis reaction of the borate network [14,17,18]. In this sense, after dissolution treatment, the glassy phase (borate) was removed and the crystals were liberated. Fig. 3 presents the microstructures

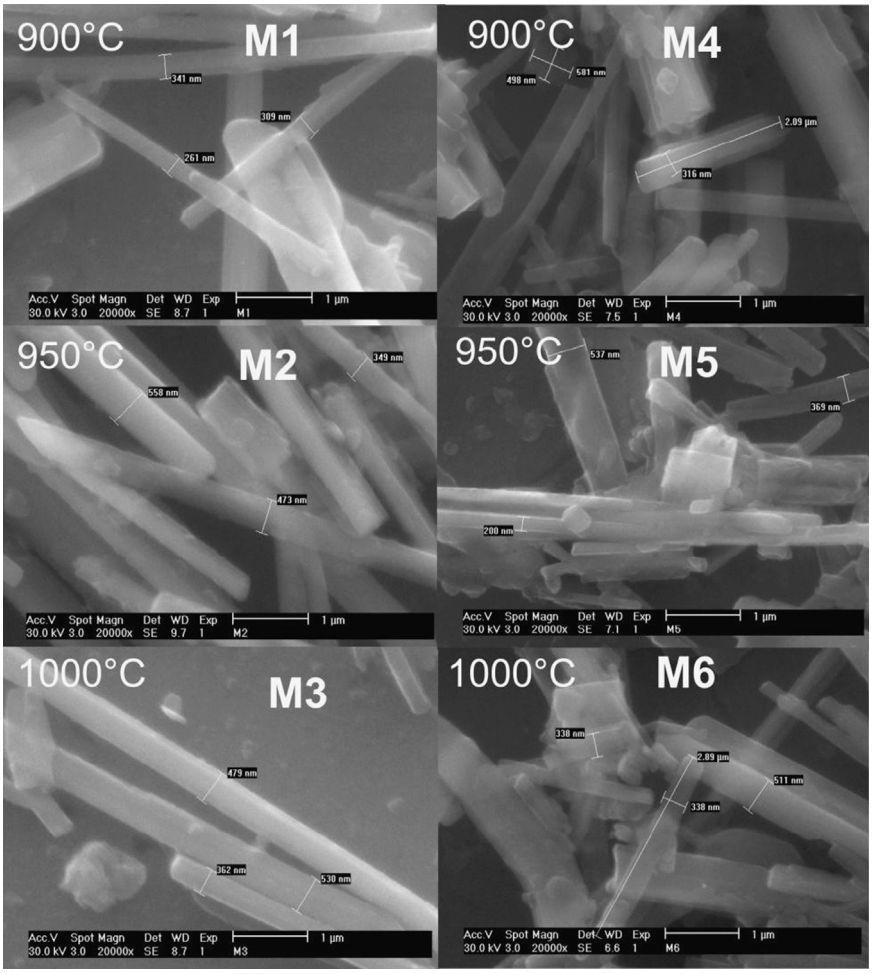

Fig. 5. Microstructures of samples M1–M6.

Table 4
Properties of the prepared $K_2Ti_6O_{13}$ samples.

Sample	Composition-heat treatment (°C)	Specific surface area (m^2/g)	Band gap (eV)	Wave length (nm)	Fiber size (µm)	
					Length	Diameter
M1	2VA1250-900	4.127	3.3	375.7	35	0.90
M2	2VA1250-950	2.811	3.3	375.7	33	0.55
M3	2VA1250-1000	2.343	3.3	375.7	12	0.53
M4	2VA1300-900	3.138	3.3	375.7	14	0.90
M5	2VA1300-950	2.607	3.3	375.7	14	0.55
M6	2VA1300-1000	2.451	3.3	375.7	20	0.51

of the samples, which did not change with the dissolution process. In all of the samples, short fibers and polygonal-like crystals can be found; however, there is a large range of sizes of the crystals of these materials, which reduces the possibility of using such materials for industrial applications.

3.2. Characterization of the heat treated samples

Fig. 4 shows the XRD results of powdered samples M1, M2, M3, M4, M5 and M6, which revealed that the crystallinity slightly increased as the temperature of the thermal treatment increased. The samples presented a defect-free acicular morphology, as shown in Fig. 5; the treatment temperature was found to not significantly influence the growth of the fiber length. However, larger diameters were observed when the temperature was increased; in addition, the sizes were homogeneous and lower than 35 µm in length and 600 nm in diameter. In addition, the samples without heat treatment were clearly found to be formless particles (Fig. 3 sample 2VA1250), whereas the samples treated thermally exhibit a needle-like shape (Fig. 4). These materials exhibited shapes and sizes similar to those obtained by the flux and calcination synthesis previously reported in the literature [2,5,19]. Likewise, a larger specific surface area of the semiconductor is usually considered to be favorable for heterogeneous catalysis because it provides more active sites for promoting the reaction. Fine single crystals of small size with fewer defects and a large specific surface area would be optimal for semiconductor photocatalysts. For this purpose, all of the samples (M1–M6) presented a large specific surface area, as listed in Table 4; an increase in the temperature of the heating treatment was found to decrease the surface area. These results are in agreement with those obtained by the XRD and SEM analyses and can be attributed to the largest crystal growth caused by the increase of the quantity of supplied

thermal energy. Similarly, obtaining smaller fibers than those reported in this paper could be expected at temperatures below 900 °C.

The DR UV–vis data of samples M1–M6 are listed in Table 3. All of the samples presented a band gap value of 3.3 eV, which is lower than the range of values of 3.52–3.60 reported by Yhosida et al. [5] and very similar to the band gap of TiO_2 (3.2 eV), which is widely used as a photocatalyst [20–22]. Given that materials with low band gap values can be activated at longer wavelengths, the synthesized potassium hexatitanate fibers can exhibit photocatalytic activity when they are irradiated with UV light at a wavelength of 375.7 nm; this finding agrees with the results reported by Manyu et al. [23], who stated that potassium hexatitanate is a lower band gap semiconductor.

4. Conclusions

Crystals of potassium hexatitanate, which melted at 1250 and 1300 °C, were produced using boric acid as a flux and different cooling methods. The amount of flux that was used enabled the generation of a liquid phase, in which the TiO_2 and K_2O reacted to form $K_2Ti_6O_{13}$, which exhibited lower crystallinity when they were cooled with water. With heat treatments at 900, 950 and 1000 °C of the samples 2VA1250 and 2VA1300, we succeeded in synthesizing $K_2Ti_6O_{13}$ fibers. Although all of the samples (M1–M6) can be used as photocatalysts due to their band gap value (3.3 eV), the fibers of sample M1 are the most promising because of its larger surface area (4.127 g/m^2) and the lower temperature used in the heating treatment (900 °C).

Acknowledgments

The authors acknowledge the Mexican programs PROMEP 103.5/12/2155 and PIFI 2014-2016 for the financial support provided for the development of this research.

References

[1] T. Zaremba, Molten salt synthesis of potassium hexatitanate, Mater. Sci. 30 (3) (2012) 180–188.
[2] N. Bao, X. Feng, L. Shen, X. Lu, Calcination syntheses of a series of potassium titanates and their morphological evolution, Cryst. Growth Des. 2 (5) (2002) 437–442.
[3] F. Xin, D. Xiaosong, S. Yijun, W. Huaiyuan, S. Shenghua, L. Xiaohua, A study on the frictional and wear behavior of polytetrafluoroethylene filled with potassium titanate whiskers, Wear 261 (2006) 1208–1212.
[4] Y. Liu, T. Qi, Y. Zhang, Synthesis of potassium hexatitante and titanium dioxide fiber by ion-exchange approach, Mater. Res. Bull. 42 (1) (2007) 40–45.
[5] H. Yoshida, M. Takeuchi, M. Sato, L. Zhang, T. Teshima, M.G. Chaskar, Potassium hexatitanate photocatalysts prepared by a flux method for water splitting, Catal. Today 232 (2014) 158–164.
[6] N. Bao, X. Lu, X. Ji, X. Feng, J. Xie, Thermodynamic modeling and experimental verification for oin-exchange synthesis of $K_2O.6TiO_2$ and TiO_2 fibers from $K_2O.4TiO_2$, Fluid Phase Equilibria 193 (2002) 229–243.
[7] G.L. Li, M. Liu, G.H. Wang, Microstructure studies of potassium hexatitanate whiskers, J. Mater. Res. 16 (2001) 12.
[8] M. Kajiwara, The formation of potassium titanate fibre with flux methods, J. Mater. Sci. 22 (1987) 1223–1227.
[9] T. Docters, J.M. Chovelon, J.M. Herrmann, J.P. Deloume, Syntheses of TiO2 photocatalysts by the molten salts method application to the photocatalytic degradation of Prosulfuron®, Appl. Catal. B 50 (2004) 219–226.
[10] K. Teshima, S.H. Lee, S. Murakoshi, S. Suzuki, K. Yubuta, T. Shishido, M. Endo, S Oishi, Highly crystalline, idiomorphic $Na_2Ti_6O_{13}$ whiskers grown from a NaCl flux at a relatively low temperature, Eur. J. Inorg. Chem. 19 (2010) 2936–2940.
[11] A.V Gorokhovsky, J.I Escalante-García, T Sánchez-Monjarás, C.A Gutiérrez-Chavarría, Synthesis of potassium polytitanate precursors by treatment of TiO_2 with molten mixtures of KNO_3 and KOH, J. Eur. Ceram. Soc. 24 (13) (2004) 3541–3546.
[12] M. Yokoyama, T. Ota, I. Yamai, Preparation of potassium hexatitanate long fibers by the flux evaporation method, J. Mater. Sci. 24 (1989) 3787–3790.
[13] M. Kajiwara, The synthesis of potassium titanate fibres by flux evaporation methods, J. Mater. Sci. 23 (1988) 3600–3602.
[14] M.A. Gonzáles-Lozano, A. Gorokhovsky, J.I. Escalante-García, Vitrification and crystallization in the system of K_2O–B_2O_3–TiO_2, J. Non-Cryst. Solids 355 (2009) 114–119.
[15] P. Pernice, S. Esposito, A. Aronne, V.N. Sigaev, Structure and crystallization behavior of glasses in the BaO–B_2O_3–Al_2O_3 system, J. Non-Cryst. Solids 258 (1999) 1–10.
[16] C.M.C. Vera, R. Aragón, Evidencia óptica de semiconducción directa en γ′-Bi_2MoO_6, Anales de la Asociación Física Argentina, Anales AFA 17 (2006) 170–172.
[17] J.M. Fernández Navarro, El Vidrio, Constitución, Fabricación, Propiedades, Consejo Superior de Investigaciones Científicas, CSIC, Madrid, 1985, pp. 133.
[18] Z. Zhang, K. Hirao, N. Soga, Water corrosion behavior of densified glass. II. Borate glasses, J. Non-Cryst. Solids 135 (1991) 62–66.
[19] J. Choy, Y. Han, A combinative flux evaporation-slow cooling route to potassium titanates fibres, Mater. Lett. 34 (1998) 111–118.
[20] Y.X. Leng, J.Y. Chen, P. Yang, H. Sun, N. Huang, The microstructure and properties of titanium dioxide films synthesized by unbalanced magnetron sputtering, Nuc. Instrum. Methods Phys. Res. Sec. B: Beam Interact. Mater. At. 257 (1-2) (2007) 451–454.
[21] A.K.P.D. Savio, D. Starikov, A. Bensaoula, R. Pillai, L.L. de la Torre García, F.C. Robles Hernández, Tunable TiO_2 (anatase and rutile) materials manufactured by mechanical means, Ceram. Int. 38 (5) (2012) 3529–3535.
[22] A.K.P.D. Savio, J. Fletcher, F.C. Robles Hernández, Sonosynthesis of nanostructured TiO_2 doped with transition metals having variable bandgap, Ceram. Int. 39 (3) (2013) 2753–2765.
[23] H. Manyu, L. Yimin, L. Chunguang, L. Xia, Structural, electronic and elastic properties of potassium hexatitanate crystal from first-principles calculations, Phys. B: Condens. Matter 407 (14) (2012) 2811–2815.